3-D Heliospheric Reconstructions From the SECCHI White Light Coronagraphs On Board STEREO: Physics and Geometry in the Reconstructions

P.A. Reiser (Interferometrics)
J.W. Cook, J.S. Newmark (Naval Research Laboratory)
P.C. Crane (Interferometrics)
A. Yahil, T. Gosnell, and R. Puetter(Pixon LLC)

The twin STEREO spacecraft will carry onboard the SECCHI (Sun-Earth Connection Coronal and Heliospheric Investigation) experiment, which consists of an EUVI disk imager and three white light coronagraphs on each spacecraft. At NRL we are investigating the tomographic electron density reconstructions, and their limitations, which are achievable from just two viewpoints using the coronagraph observations.

In this presentation we discuss the physics and geometry used in our PIXON reconstruction technique. As part of our technique, we must mathematically calculate (render), from a given electron density distribution in space, a synthetic white light image of the electron-scattered K corona along a chosen line-of-sight from the center of the solar disk to the center of the synthetic image. We discuss the physics of Thomson scattering of photospheric light from coronal electrons, in radial and tangential polarizations. The geometry we have implemented includes the observer at a finite distance from the Sun, not at infinity, and a model Sun with full limb darkening treatment. Our reconstruction technique must be sufficiently robust and general in its geometric basis to handle not just the Sun-centered Cor 1 and Cor 2 coronagraphs, but also the HI (Heliospheric Imager) coronagraph which observes outward along the Sun-Earth line, introducing more demanding reconstruction considerations.

This work is supported by NASA under S-13631-Y, and by the Office of Naval Research. The SECCHI experiment is an international collaboration lead by the Naval Research Laboratory.

STEREO

The SECCHI[1] coronagraphs will be carried on board the two STEREO spacecraft in solar orbit. They will each view the solar K-corona from a different angle. One spacecraft will be ahead of the earth in its orbit around the sun, the other will be behind. The overlapping viewpoints will allow a clearer picture of the solar K-corona to be obtained.

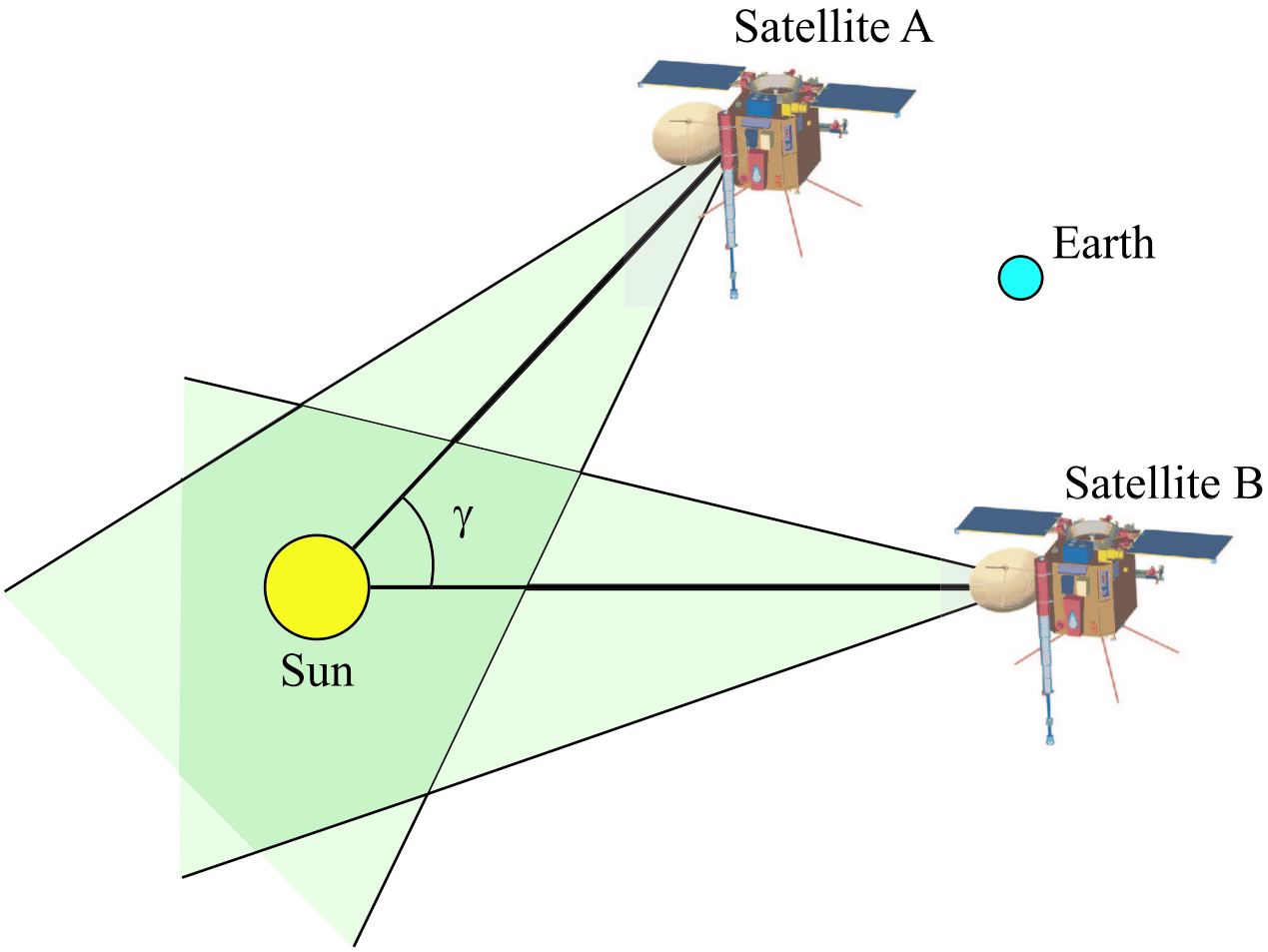

Figure 1: STEREO Spacecrafts and the Sun

In order to reconstruct the electron density from the image of the K-corona captured by the spacecrafts, we must be able to:

- Calculate the radiance at each spacecraft due to the scattered radiation from any line of sight viewed by the spacecraft
- Calculate the position of that line of sight on the detector of each spacecraft.

Thomson Scattering

The solar K-corona arises from Thomson scattering of solar photons from hot coronal electrons. The scattered radiation is polarized, and is dependent upon the scattering angle χ. The following diagram defines the relevant parameters for Thomson scattering from a point source

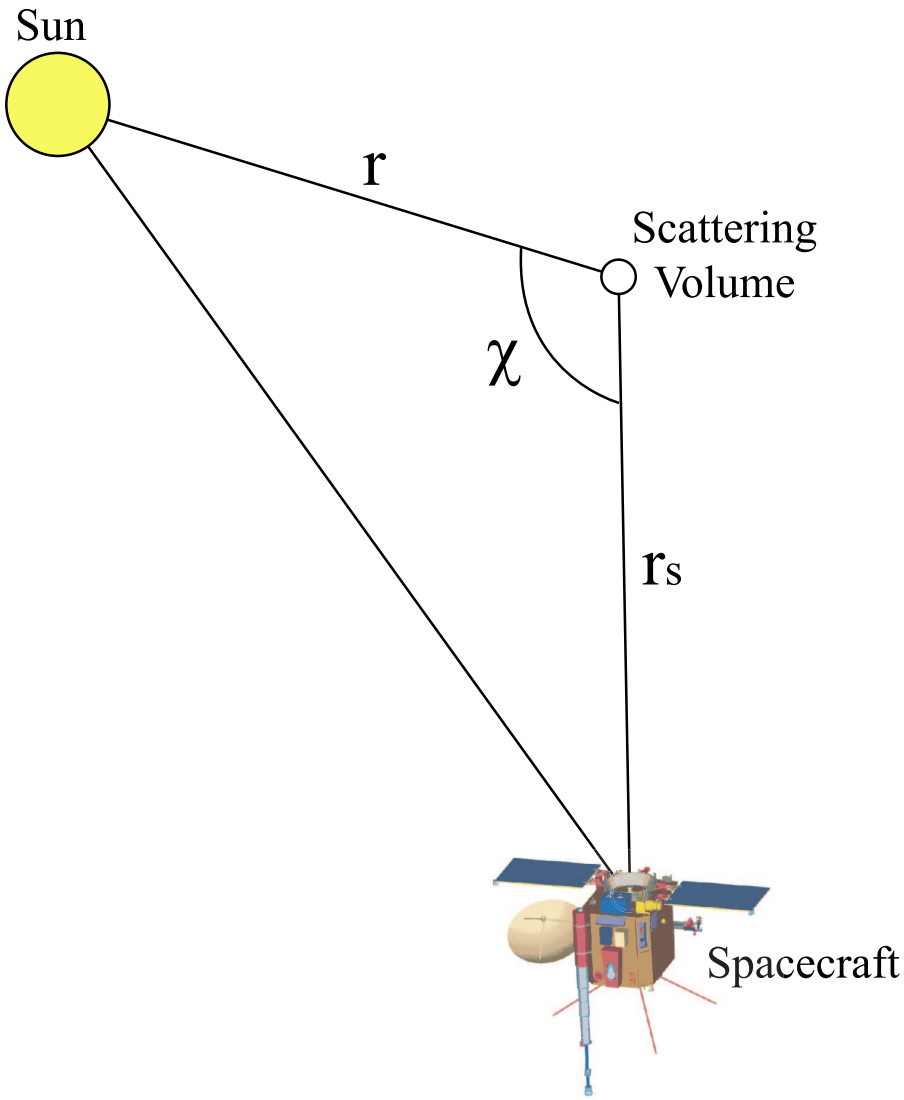

Figure 2: Geometry for Thomson Scattering

The fact that the sun is actually an extended source will modify the physics of the scattering process. Qualitatively the effect will be to reduce the degree of polarization of the scattered radiation

Emission Coefficient

We separate the scattered radiation into tangentially and radially polarized light. The tangential emission coefficient (photons $\sec^{-1}$ cm^{-3} sr^{-1}) may be written:[2]

$$\epsilon_t(\boldsymbol{r}) = \frac{\pi I_0 \sigma}{2}\, n_e(\boldsymbol{r})\, \Sigma_A$$

and the radial emission coefficient may be written:

$$\epsilon_r(\boldsymbol{r}) = \frac{\pi I_0 \sigma}{2}\, n_e(\boldsymbol{r})\, (\Sigma_B\ \cos^2(\chi_s) + \Sigma_C)$$

where I_0 is the solar intensity at disc center, R is the solar radius, r is the distance of the scattering point from sun center, σ is the Thomson scattering cross section, χ_s is the scattering angle, and Σ_A, Σ_B, and Σ_C, are functions of r/R which account for the non-zero radius of a limb-darkened sun[2, 4, 3, 5].

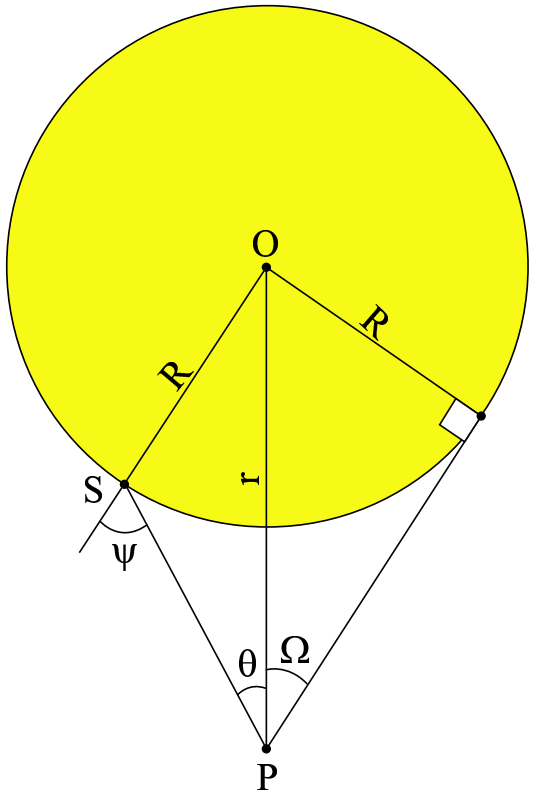

Figure 3: Definition of Angles for Limb Darkening

Polynomial Limb Darkening

The Σ-coefficients are defined as[2]:

$$\begin{aligned}
\Sigma_A &\equiv \int_{\cos(\Omega)}^{1} L(\theta)\left[\cos^2(\theta)+1\right] d\cos(\theta) \\
\Sigma_B &\equiv \int_{\cos(\Omega)}^{1} L(\theta)\left[3\cos^2(\theta)-1\right] d\cos(\theta) \\
\Sigma_C &\equiv \Sigma_A - \Sigma_B
\end{aligned}$$

where $L(\theta)$ is the limb darkening function. We may approximate the limb darkening function by a polynomial[6] in $\cos(\psi)$[1]:

$$L(\theta) = \sum_{n=0}^{N} a_n \ \cos^n(\psi)$$

The Σ coefficients now become:

$$\begin{aligned}
\Sigma_A &= \sum_{n=0}^{N} a_n A_n(\Omega) \\
\Sigma_B &= \sum_{n=0}^{N} a_n B_n(\Omega)
\end{aligned}$$

where:

$$\begin{aligned}
A_n &\equiv \int_{\cos(\Omega)}^{1} \left[\cos^2(\theta)+1\right] \cos^n(\psi) d\cos(\theta) \\
B_n &\equiv \int_{\cos(\Omega)}^{1} \left[3\cos^2(\theta)-1\right] \cos^n(\psi) d\cos(\theta)
\end{aligned}$$

These integrals may be solved to yield analytic expressions for the Σ coefficients for any N. We may also derive the following expression relating the mean and central solar intensity.

$$\frac{I_m}{I_0} = 1 - \sum_{n=1}^{N} \frac{n\ a_n}{n+2}$$

[1] In order to assure that L(0)=1, the a_n are constrained by:

$$\sum_{n=0}^{N} a_n = 1$$

Spacecraft Measurement of Scattered Radiation

Now that we have the emission coefficient for a volume element, we will want to determine the number of photons collected by a pixel of the spacecraft's CCD detector. Since the K-corona is optically thin, this will be the sum of the contributions of all volume elements "seen" by that pixel.

Assuming the angle of incidence to the camera is small, the total number of photons contributed by a volume element dV may be written:

$$dN = aT\frac{\epsilon(\boldsymbol{r})\ dV}{r_s^2}$$

where a is the aperture area and T is the exposure time. The total number of photons at that point on the detector will be the integral along the entire line of sight (C):

$$N = aT\ \int_C \frac{\epsilon(\boldsymbol{r})}{r_s^2}\ dV \tag{6.1}$$

Defining τ as the plate scale (radians per pixel), we may also write the number of photons striking a pixel as:

$$N = aT\ \tau^2 \int_C \epsilon(\boldsymbol{r})\ dl \tag{6.2}$$

but in order to accomplish this integration, we must determine the path length through a voxel and determine whether the voxel is wholly or partially in the field of view of the pixel. This is computationally less convenient than Equation 6.1.

The Rendering Process

The electron density will be approximated by a cubic array of voxels. It will be assumed that the scattered radiation from a voxel can be approximated by a point source located at the center of the voxel. This will allow a simplification of the rendering process. Having determined the flux at each imaged point on the detector, we now want to find the position of that imaged point on the detector. In order to simplify things, we will consider the imaging system of each spacecraft to be a pinhole camera.

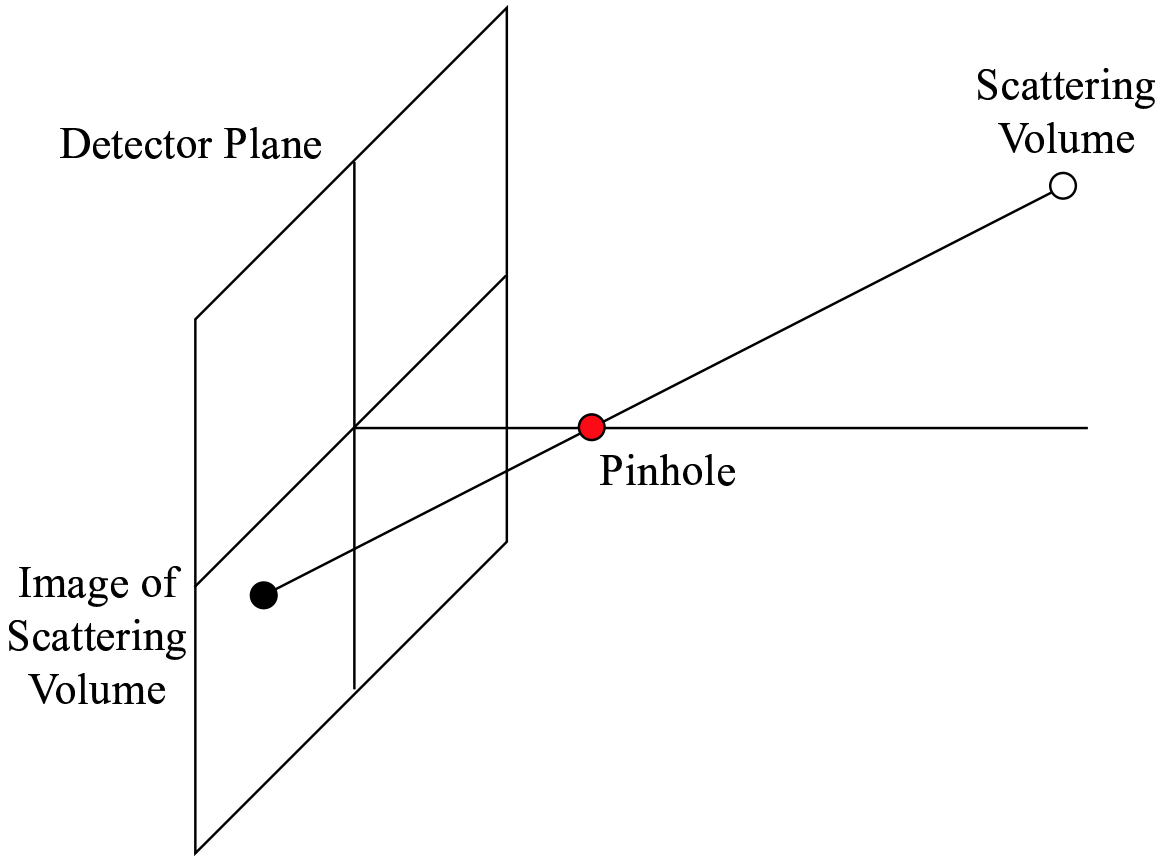

Figure 4: Imaging of Scattering Volume by Pinhole Camera

To a first approximation, we may consider the response of a pixel in the detector to be the sum of the contributions of all voxels whose centers are imaged inside that pixel.

Coordinate Systems

In order to calculate the position and intensity of a voxel image on the detector, a number of geometric parameters are required. Some of these parameters are very simply expressed in certain coordinate systems, others are better expressed in other coordinate systems. There are a total of five coordinate systems which have been found useful in this development. They are:

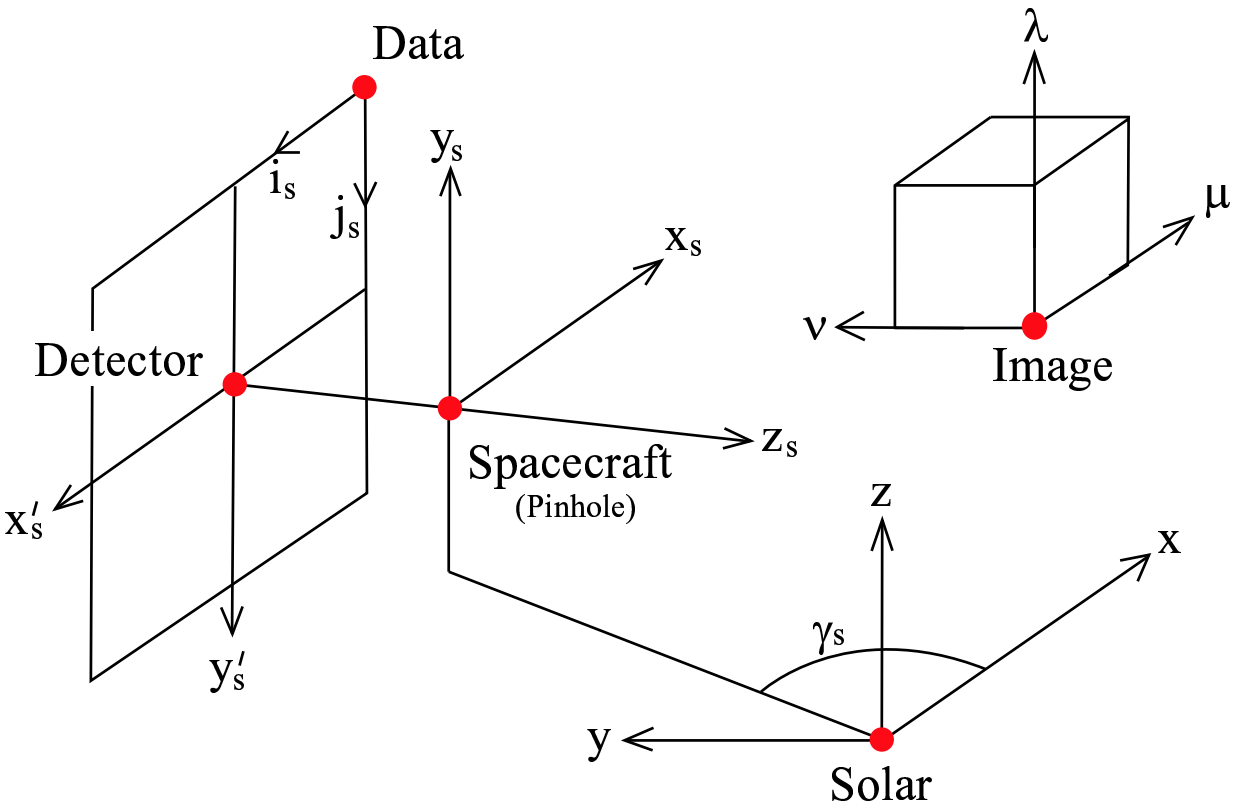

Figure 5: The Five Coordinate Systems

- The image coordinate system (μ, ν, λ)
- The solar coordinate system (x, y, z)
- The spacecraft coordinate system (x_s, y_s, z_s)
- The detector coordinate system (x'_s, y'_s)
- The data coordinate system (i_s, j_s)

Projective Geometry

The formalism of Projective Geometry[7, 8] is especially useful in analyzing the rendering process. As an example of its usefulness, consider the affine transformation. We will want to transform between the various coordinate systems described above. These coordinate systems are all related by affine transformations. The vector $\boldsymbol{r'}$ is related to vector $\boldsymbol{r}$ by an affine transformation if:

$$\boldsymbol{r'} = \boldsymbol{T}\boldsymbol{r} + \boldsymbol{r_0}$$

where $\boldsymbol{T}$ is a linear vector operator. For 3-dimensional vectors, this relationship may be written in matrix notation as:

$$\begin{bmatrix} x' \\ y' \\ z' \end{bmatrix} = \begin{bmatrix} R_{00} & R_{01} & R_{02} \\ R_{10} & R_{11} & R_{12} \\ R_{20} & R_{21} & R_{22} \end{bmatrix} \begin{bmatrix} x \\ y \\ z \end{bmatrix} + \begin{bmatrix} x_0 \\ y_0 \\ z_0 \end{bmatrix}$$

Projective geometry represents 3-dimensional points in a real Euclidean space as 4-dimensional arrays with an equivalence relationship ($\cong$) such that $\boldsymbol{r} \cong \lambda\boldsymbol{r}$ where λ is a real number $\neq 0$. In projective geometry terms, we may represent the above affine transformation as:

$$\begin{bmatrix} x' \\ y' \\ z' \\ 1 \end{bmatrix} = \begin{bmatrix} R_{00} & R_{01} & R_{02} & x_0 \\ R_{10} & R_{11} & R_{12} & y_0 \\ R_{20} & R_{21} & R_{22} & z_0 \\ 0 & 0 & 0 & 1 \end{bmatrix} \begin{bmatrix} x \\ y \\ z \\ 1 \end{bmatrix}$$

In other words, the affine transformation in 3-space becomes a linear transformation in projective space. All of the conceptual simplicity and advantages of linear analysis can be brought to bear on the Euclidean space by treating it as a projective space. This is just one example of the many ways in which projective geometry will be found useful.

Coordinate Transformations

The 5 coordinate systems will require 4 transformations to link them. Defining $\mathbf{\Lambda} = [\mu, \nu, \lambda]$ as the image coordinates, with $\mathbf{\Lambda}_0$ being the image coordinates of the sun, the transformation linking solar coordinates ($\boldsymbol{r} = [x, y, z]$) to image coordinates is:

$$\begin{bmatrix} x \\ y \\ z \\ 1 \end{bmatrix} \cong \begin{bmatrix} 1 & 0 & 0 & \text{-}\mu_0 \\ 0 & 1 & 0 & \text{-}\nu_0 \\ 0 & 0 & 1 & \text{-}\lambda_0 \\ 0 & 0 & 0 & 1/d \end{bmatrix} \begin{bmatrix} \mu \\ \nu \\ \lambda \\ 1 \end{bmatrix} \quad or \quad \boldsymbol{r} = \boldsymbol{W}\mathbf{\Lambda}$$

For a spacecraft pointing at the sun, at angle γ to the x-axis, a distance of L from the sun, the transformation linking spacecraft coordinates ($\boldsymbol{r}_s = [x_s, y_s, z_s]$) to solar coordinates is:

$$\begin{bmatrix} x_s \\ y_s \\ z_s \\ 1 \end{bmatrix} = \begin{bmatrix} S_\gamma & -C_\gamma & 0 & 0 \\ 0 & 0 & 1 & 0 \\ -C_\gamma & -S_\gamma & 0 & L \\ 0 & 0 & 0 & 1 \end{bmatrix} \begin{bmatrix} x \\ y \\ z \\ 1 \end{bmatrix} \quad or \quad \boldsymbol{r_s} = \boldsymbol{R}\boldsymbol{r}$$

Defining h as the distance from the aperture to the detector plane, the transformation linking detector coordinates ($\boldsymbol{r'}_s = [x'_s, y'_s)$ to spacecraft coordinates is:

$$\begin{bmatrix} x'_s \\ y'_s \\ 1 \end{bmatrix} \cong \begin{bmatrix} h & 0 & 0 & 0 \\ 0 & h & 0 & 0 \\ 0 & 0 & 1 & 0 \end{bmatrix} \begin{bmatrix} x_s \\ y_s \\ z_s \\ 1 \end{bmatrix} \quad or \quad \boldsymbol{r'_s} = \boldsymbol{P}\boldsymbol{r_s}$$

Defining k as the length of the side of a pixel, the transformation linking data coordinates ($\boldsymbol{k} = [i_{0s}, j_{0s}]$) to detector coordinates is:

$$\begin{bmatrix} i_s \\ j_s \\ 1 \end{bmatrix} = \begin{bmatrix} 1/k & 0 & i_0 \\ 0 & 1/k & j_0 \\ 0 & 0 & 1 \end{bmatrix} \begin{bmatrix} x'_s \\ y'_s \\ 1 \end{bmatrix} \qquad or \quad \boldsymbol{k} = \boldsymbol{V_s}\boldsymbol{r'_s}$$

Finally, the transformation linking image coordinates to data coordinates is just the product of the transformations:

$$\boldsymbol{k} \cong (\boldsymbol{V}_s\boldsymbol{P}\boldsymbol{R}_s\boldsymbol{W})\mathbf{\Lambda} \equiv \boldsymbol{G}\mathbf{\Lambda} \tag{10.3}$$

The PIXON Method

We are using the PIXON method[9, 10, 11, 12] to estimate the electron density distribution from the images of the K-Corona measured by the two STEREO spacecrafts. Although in principle, there are an infinite number of solutions to this tomography problem, the PIXON method seeks a solution which has minimum complexity. It does so by smoothing the image model locally as much as the data allow, thus reducing the number of independent patches or "pixons" in the image. A block diagram of the PIXON program is shown below:

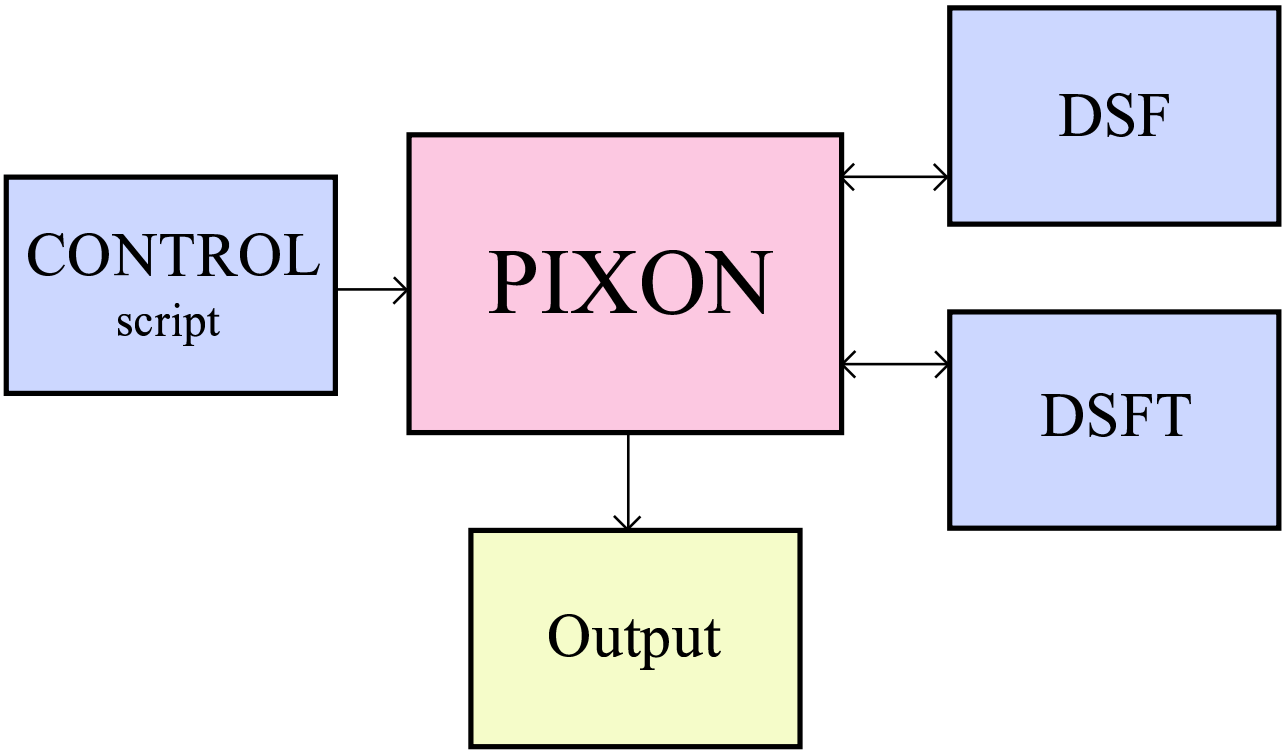

Figure 6: PIXON Block Diagram

One of the primary requirements of the PIXON software package is that the *Data Sampling Function* (DSF) be specified. This essentially takes as input the 3-D electron density image, and renders it to a 2-D image of the Thomson scattered radiation. An associated program, called the DSFT function, is essentially the transpose of the DSF function, taking an input data image and back-projecting onto the electron density cube.

The Data Sampling Function (DSF)

The DSF renders the electron density into an image of the scattered radiation. Define $dN_{\mu\nu\lambda}$ as the number of photons striking the detector which originate from voxel $\mu\nu\lambda$. We may write the total number of photons striking pixel i, j as N_{ij} where:

$$N_{ij} = \sum_{\mu\nu\lambda} \Phi_{ij;\mu\nu\lambda}\ dN_{\mu\nu\lambda}$$

where $\Phi_{ij;\mu\nu\lambda}$ is the rendering function and specifies the fraction of the photons from voxel $\mu\nu\lambda$ which land on pixel ij. [2]

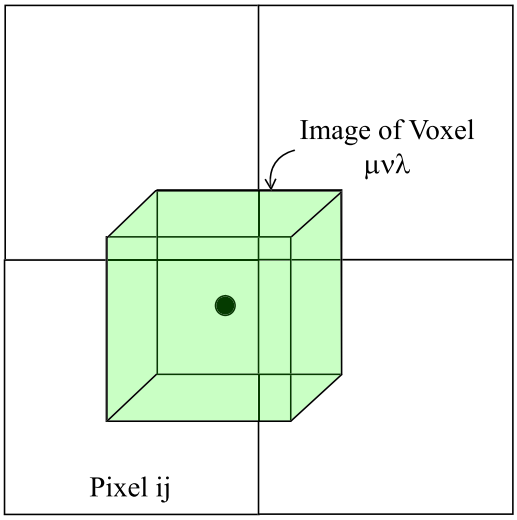

Figure 7: Image of a Voxel on the Detector

Since the number of photons detected is proportional to the electron density, we may write the $dN_{\mu\nu\lambda}$ as:

$$dN_{\mu\nu\lambda} = Q_{\mu\nu\lambda}\ n_{\mu\nu\lambda}$$

where $Q_{\mu\nu\lambda}$ is the proportionality constant relating the integrated flux to electron density. This allows the integrated flux to be written in terms of the data sampling function (DSF) $H_{ij;\mu\nu\lambda}$:

$$F_{ij} = \sum_{\mu\nu\lambda} \Phi_{ij;\mu\nu\lambda}\ Q_{\mu\nu\lambda}\ n_{\mu\nu\lambda} = \sum_{\mu\nu\lambda} H_{ij;\mu\nu\lambda}\ n_{\mu\nu\lambda}$$

[2] As an example, a very simple rendering function is to assign all photons from a voxel to whatever pixel the point at the center of the voxel images to:

$$\Phi_{ij;\mu\nu\lambda} = \Delta(\boldsymbol{K}_{ij} - [\boldsymbol{G}\boldsymbol{\Lambda}_{\mu\nu\lambda}])$$

where $\boldsymbol{K} \equiv [i, j, 1]$ (i and j are integers), $\boldsymbol{\Lambda} \equiv [\mu, \nu, \lambda, 1]$, $\boldsymbol{G}$ is the transformation operator defined in Equation 10.3, and $\Delta(x)$ is the Kronecker delta function. The brackets represent the "nearest integer" function.

An Example

As an example of the PIXON solution to a given set of data images, we have 'invented' a solar CME which consists of half of a spherical shell whose axis of symmetry contains the sun. The "true" and reconstructed images are shown below:

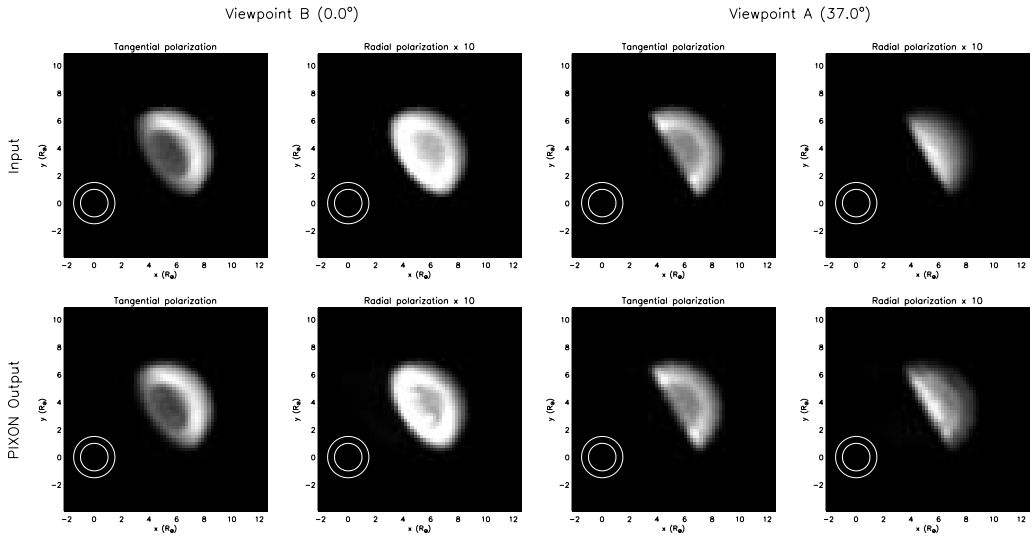

Figure 8: "True" and Reconstructed Rendered Data

Projections of the "true" and reconstructed electron density are shown in the figure below:

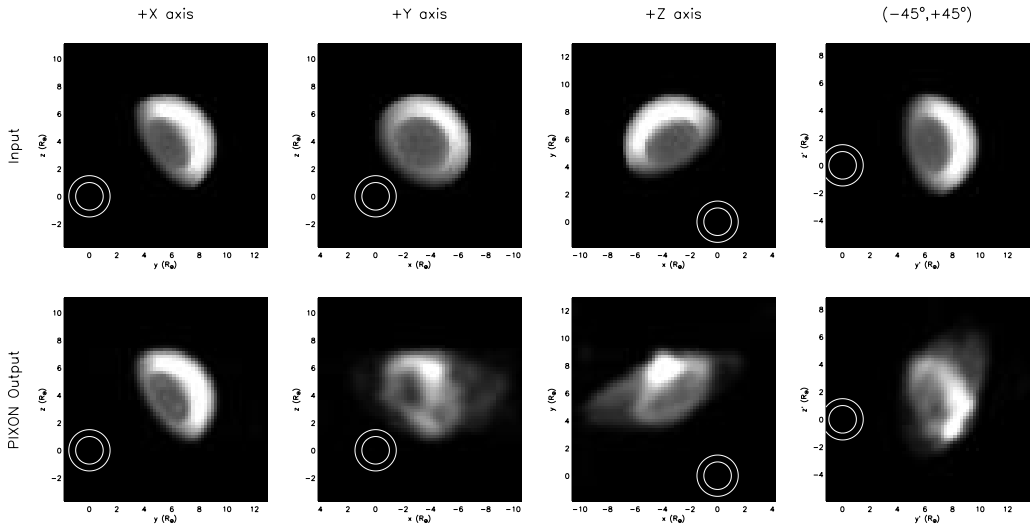

Figure 9: "True" and reconstructed Electron Density

References

[1] Russell A. Howard, J. Daniel Moses, Dennis G. Socker, "Sun Earth Connection Coronal and Heliospheric Investigation (SECCHI)", Proc. SPIE Vol. 4139, p. 259-283

[2] Billings, Donald E., "A Guide to the Solar Corona", Academic Press, New York 1966.

[3] Minnaert, M., Z.f. Ap. **1**, 209, 1930.

[4] van de Hulst, H. C. 1950, Bull. Astron. Inst. Netherlands, 11 (410), 135

[5] Milne, E.A., 1921, MNRAS 81, pp361-375.

[6] Neckel, H. and Labs, D., "Solar Limb Darkening" 1986-1990 Solar Physics 153:91-114, 1994.

[7] Faugeras, Stratification of three-dimensional vision: projective, affine, and metric representations, Journal of the Optical Society of America, 1995.

[8] Shashua, Amnon, "On Geometric and Algebraic Aspects of 3D Affine and Projective Structures from Perspective 2D Views", A.I. Memo No 1405, Massachusetts Institute of Technology Artificial Intelligence Laboratory and Center for Biological Computational Learning, Whitaker College, July, 1993.

[9] Puetter, R.C.: 1995,"Pixon-Based Multiresolution Image Reconstruction and the Quantification of Picture Information Content," Int. J. Image Sys. & Tech. 6, 314-331.

[10] Puetter, R.C.: 1996, "Information, Language, and Pixon-Based Bayesian Image Reconstruction in Digital Image Recovery and Synthesis III", P.S. Idell, and T.J. Schulz, eds., Proc. S.P.I.E 2827, 12-31.

[11] Puetter, R.C.: 1997, "Modern Methods of Image Reconstruction," Instrumentation for Large Telescopes, J.M. Rodriguez Espinosa, A. Herrero, and F. Sanchez, eds., Cambridge University Press, New York, 75-122.

[12] Puetter, R.C., and Yahil, A.: 1999, "The Pixon Method of Image Reconstruction," in Astronomical Data Analysis Software and Systems VIII, D.M. Mehringer, R.L. Plante, and D.A. Roberts, eds., ASP Converence Series 172, 307-316.

[13] Davila, J.E., "Solar Tomography", Astophys. J. 1994 **423**, 871.

[14] Gary, G. Allen, Davis, John M. and Moore, Ronald, "On Analysis of Dual Spacecraft Stereoscopic Observations to Determine the Three Dimensional Morphology and Plasma Properties of Solar Coronal Flux Tubes", Submitted to Solar Physics.